Journal of Applied Polymer Science

Comparison of the Adsorption Behavior of Flavonoids on Three Macroporous Adsorption Resins Modified with Hydrogen-Bond Groups

Helin Ye,[1,2,3] Zhenbin Chen,[4] Yongfeng Liu,[1,2,3] Song Lou,[1,2,3] Duolong Di[1,2]

[1]Key Laboratory of Chemistry of Northwestern Plant Resources, Lanzhou Institute of Chemical Physics, Chinese Academy of Sciences, Lanzhou 730000, People's Republic of China

[2]Key Laboratory for Natural Medicine of Gansu Province, Lanzhou Institute of Chemical Physics, Chinese Academy of Sciences, Lanzhou 730000, People's Republic of China

[3]Graduate University, Chinese Academy of Sciences, Beijing 100049, People's Republic of China

[4]State Key Laboratory of Gansu Advanced Nonferrous Metal Materials, Lanzhou University of Technology, Lanzhou 730050, China

Correspondence to: D. Di (E-mail: didl@licp.cas.cn)

ABSTRACT: Three macroporous crosslinked poly(styrene-*co*-divinyl benzene) resins functionalized with *p*-phenylene diamine (PPDA), *p*-aminophenol, and *p*-aminobenzoic acid (PANB) groups were prepared, and their adsorption characteristics for the flavonoid constituents from the leaves of *Olea europaea L* were studied. The materials were characterized by Fourier transform infrared spectroscopy. The specific surface area and the pore size distribution of the adsorbents were calculated by the Brunauer–Emmett–Teller and Barrett-Joyner-Halenda methods. The results show that the materials had a faster adsorption rate and high adsorption capacities for flavonoids, and PPDA had the highest adsorption capacity in comparison with the others. The isotherms could be fitted by the Freundlich model, and the adsorption was an exothermic process. The adsorption kinetics could be characterized by the pseudo-second-order rate equation, and the initial stage was controlled by the intraparticle diffusion model. This study contributes to the remediation of adsorption for organic materials and active components of natural products and to the effects of different functional groups on adsorption mechanisms. © 2013 Wiley Periodicals, Inc. J. Appl. Polym. Sci. **2014**, *131*, 40188.

KEYWORDS: adsorption; applications; addition polymerization

Received 5 November 2012; accepted 6 November 2013
DOI: 10.1002/app.40188

INTRODUCTION

Macroporous adsorption resins (MARs) are viewed as attractive alternatives for separating organic compounds because of their high efficiency, low pollution, and procedural simplicity. They have been used extensively in many fields, including chromatographic analysis,[1] medical treatments,[2] and wastewater disposal.[3] Except for the general advantage as that of a common adsorbent, MARs possess more favorable properties, including their structural diversity and low cost, which make them more promising.[4] However, these MARs often have low adsorption capacities (q_e; mg/g) and adsorption selectivity for the adsorption of organic compounds. To gain greater q_e and higher adsorption selectivity for some specific organic compounds, the chemical modification of MARs is often adopted by the introduction of special functional groups into the matrix of the polymeric adsorbents;[5,6] this changes the chemical composition of the adsorbent surface and, hence, improves its adsorption for organic compounds.[7] Until now, some specific functional groups, such as amino, amide, hydroxyl, carbonyl, and carboxyl groups, have been introduced onto the surface of the resin.[8–11] Because of the adsorption restriction and the competition among the adsorbates, the adsorption feature of MARs has not been sufficiently explored. Moreover, instead of investigating the adsorption features of MARs systemically, previous researchers[12–15] simply attributed the adsorption of MARs to the hydrogen-bonding effect. The matrix of these MARs was usually a polyacrylic or styrene–divinyl benzene ester. The adsorption mechanism of MARs primarily relies on a hydrophobic force, such as van de Waal's forces in the aqueous solution, which may lead to the low adsorption selectivity. As a result, the state of theoretical research has not improved, and this has resulted in a lack of information on molecular design in the synthesis and modification process of MARs and has further hampered the development of research and applications on MARs.

There have been some reports on the application of the commercial MARs in the enrichment process of flavonoids.[16–18] In previous studies in our laboratory,[19,20] we systematically studied the

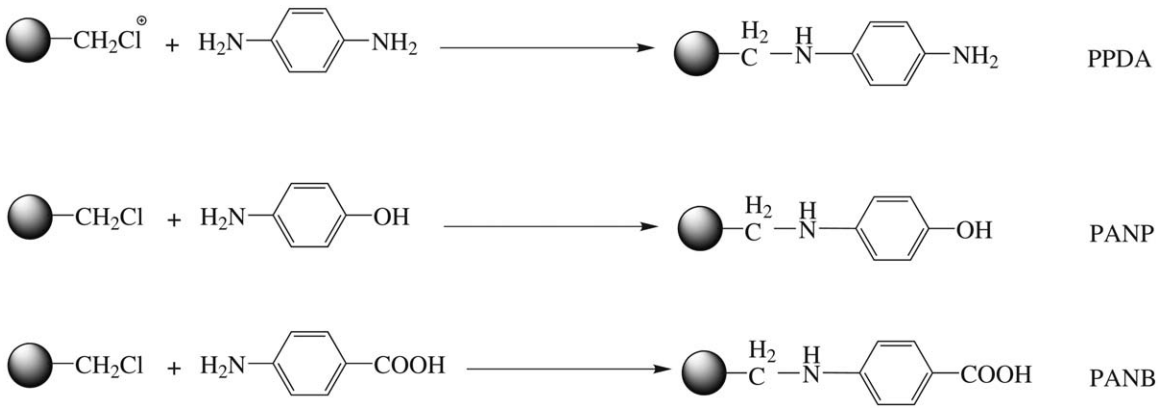

Scheme 1. Preparation of the three modified resins.

preparative separation and purification of flavonoids from *Olea europaea L.* leaves by eight commercial-mode MARs.[21] However, little has been done to compare the adsorption capacity of resins with different hydrogen-bonding groups or to determine the impact of the pore size distribution. An understanding of these features will benefit the development of an efficient, successful purification process. In this study, three types of MARs with novel matrices and hydrogen-bonding groups were prepared (in Scheme 1). The adsorption behavior of three new polymeric adsorbents, in a macroporous styrene-*co*-divinyl benzene copolymer with chloromethyl groups (DDM1) chemically modified with *p*-phenylene diamine (PPDA), *p*-aminophenol (PANP), and *p*-aminobenzoic acid (PANB), for flavonoids from the extract of leaves of Olea europaea L (LOL) were investigated. The adsorption isotherms of flavonoids onto these adsorbents were measured and correlated to Langmuir and Freundlich isotherms. With the help of the adsorption enthalpies[22,23] and the adsorption behaviors of polymeric adsorbents for total flavonoids, the adsorption mechanism was explained. Through a comparison of the adsorption behaviors of the three functionalized macroporous resins, the influence of different functional groups drew our attention. Furthermore, our interest was also focused on the adsorption of MARs to flavonoids from LOL, and the influence of matching degrees of the structural parameters with respect to synthetic MARs and flavonoids and the adsorption feature.

EXPERIMENTAL

Materials

The initial beads, which were non-polar styrene-co-divinylbenzene copolymer (DDM-0) with no functional groups, were purchased from Sunrisin Technology Co., Ltd. (Xi'an, China). Analytical-grade ethanol, methanol, sodium chloride, dichloromethane, *N,N*-dimethylformamide (DMF), PPDA, PANP, PANB, zinc chloride, and sodium chloride were purchased from Tianjin Chemical Reagent Co., Inc. (Tianjin, China). Pharmaceutical-grade chloromethyl methyl ether was purchased from Jinan Leqi Chemical Reagent Co., Inc. (Shandong, China), and distilled water was used.

O. europaea L. leaves were obtained from Gansu Greenness Biotech Co., Ltd. (Gansu, China) and were used after they were washed and dried. Standards were purchased from the National Institutes for Food and Drug Control (Beijing, China).

Instruments

A Sartorius BT224S analytical balance (Sartorius Scientific Instruments Co., Ltd., Beijing, China), a mechanical magnetic stirrer, a reflux condenser, a thermometer, a rotary evaporator (RE-52C, Gongyi City Yuhua Instrument Co., Ltd., China), a Fourier transform infrared (FTIR) spectrometer (Nicolet), a Micromeritics ASAP 2020 automatic surface area and porosity analyzer (Micromeritics Instrument Corp.), a SHA-B incubator (100 rpm, Jintan Zhengji Instrument Co., Ltd., Jiangsu Province, China), and a UV spectrometer (T-6, Beijing Purkinje General Instrument Co., Ltd., Beijing, China).

Preparation of the Polymeric Adsorbents

MARs with chloromethyl groups were prepared with an electrophilic substitution method. The initial beads (MARs of PSs with no functional groups) were soaked in dichloromethane for 24 h after they were filtered and ready to be used. Then, the soaked MARs were chloromethylated with 150 mL of monochloromethyl ether, and anhydrous zinc chloride (12 g) was used as the catalyst and was added to the reaction vessel in two batches. After the first 6 g of anhydrous zinc chloride was dissolved in the solution at room temperature, the second batch was added, and the reaction temperature was increased to 311 K within 0.5 h after the catalyst was dissolved. The reaction was retained for about 20 h until the chlorine content of the polymeric beads reached 3.55 mmol/g, and thus, chloromethylated PS was prepared.

The synthesized chloromethylated PSs were divided in three equal batches to react thereafter to make the base chlorine contents equal.

The synthesis of PPDA was performed as below: 20 g of chloromethylated PS was swollen with 150 mL of DMF overnight in a round-bottomed flask; by amination, it was treated with 0.76 g of PPDA in 200 mL of DMF. The resulting mixture was shaken at 343 K for 12 h. After the reaction was finished, the solid particles were filtered from the solution, rinsed in methanol, and washed with dichloromethane, acetone, ethanol, and deionized water. Finally, the purple particles were obtained.

With regard to the synthesis of PANP, 20 g of chloromethylated PS was swollen with 150 mL of DMF overnight in a round-

bottomed flask. Then, 0.77 g of PANP was added. The reaction solution was kept at 353 K for about 10 h until the reaction was finished. The resulting polymeric beads were washed with distilled water, extracted with dichloromethane, acetone, absolute alcohol, and dried at 323 K *in vacuo*. Thus, the PANP-modified PS resin was obtained, and the color of the particles was brown.

As far as the preparation of PANB was concerned, 20 g of chloromethylated PS was swollen with 150 mL of DMF overnight in a round-bottomed flask, and PANB was added as the reacting reagent. The reaction was kept at 343 K for 12 h, and PANB was achieved. The resulting product was washed with distilled water; extracted with dichloromethane, acetone, and ethanol; and dried at 323 K *in vacuo*. The resulting particles were pale yellow.

Characterization of the Polymeric Adsorbents

The chlorine content of the chloromethylated PS, PPDA, PANP, and PANB was determined with the Volhard method. The specific surface area of the adsorbents was measured by a Micromeritics ASAP 2020 surface area measurement instrument according to the Brunauer–Emmett–Teller (BET) method. The IR spectra of the adsorbents were achieved by a Nicolet 510P FTIR instrument.

Preparation of the Sample Solutions

The *O. europaea L.* leaves (1 kg) were extracted with 3 L of 70% ethanol in a bath at 353 K for 2 h; this was repeated with 2 L of 70% ethanol. The double extracts were mixed and negative-pressure filtered, and then, the filtrate was evaporated to yield the fluid extract by the removal of the ethanol under reduced pressure in a rotary evaporator at 323 K. The extract of *O. europaea L.* leaves was photophobically stored in a refrigerator at 253 K. Then, the extract was thawed at ambient temperature before use and diluted to an appropriate concentration with distilled water to produce the sample solutions.

Measurement of the Adsorption and Desorption Isotherms

Equilibrium adsorption of the total flavonoids on the three polymeric adsorbents in the sample solution was performed at 298, 308, and 318 K, respectively. Accurately weighed dry adsorbent (1.00 g) was directly introduced into a 250-mL conical flask. Then, 100 mL of a sample solution with known concentration [C_0 (mg/L)] was added to each flask. The flasks were completely sealed and shaken in a thermostatic oscillator at a predetermined temperature for about 8 h until equilibrium was reached. The equilibrium concentration of total flavonoids [C_e (mg/L)] was determined. C_e in the drain was analyzed with a UV spectrophotometer. The experiments of desorption were carried out as follows: 100 mL of ethanol (70% v/v) was pumped into a flask with the adsorbate-laden MARs after the adsorption reached equilibrium. The flask was shaken (100 rpm) at a constant temperature of 303 K for 6 h. Then, the corresponding concentration of flavonoids (concentration of desorbed solution) was analyzed with a UV spectrophotometer. The q_e values of the total flavonoids were calculated according to eq. (1):

$$q_e=(C_0-C_e)V/W \tag{1}$$

where V is the volume of the total flavonoid solution (L) and W is the weight of macroporous resins (g). The adsorption isotherms of the total flavonoids onto PPDA, PANP, and PANB were derived in the sample solution accordingly.

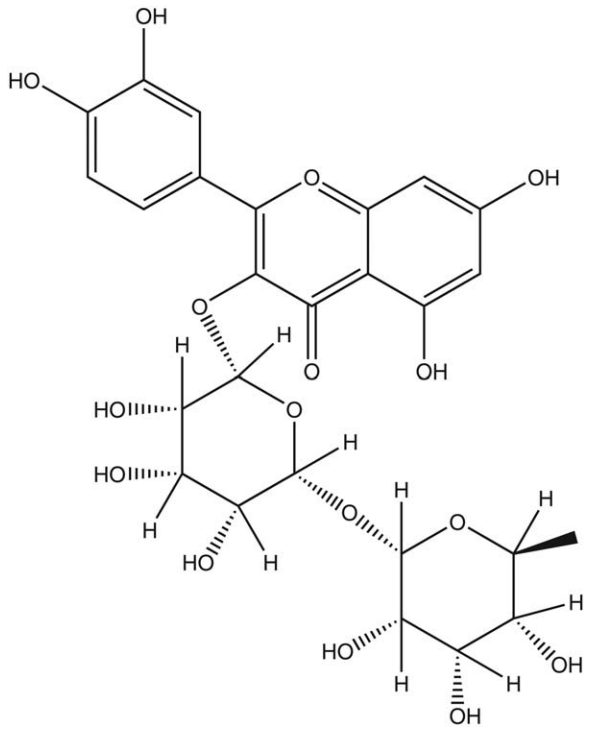

Scheme 2. Structure of rutin.

The desorption capacity of the total flavonoids (q_e'; mg/g) was calculated as follows:

$$q_e'=C_e'V/W \tag{2}$$

where C_e' is the equilibrium concentration of desorption.

Determination of the Total Flavonoid Content

The total flavonoid content was determined with a colorimetric method. The sample solution (1 mL) diluted by an ethanol solution (30% v/v) to 5 mL; then, 4 mL of $AlCl_3$ solution (1%) was added. The final volume was adjusted to 10 mL with an ethanol solution (30% v/v). The mixture was allowed to stand for 10 min, and the absorption was measured at 415 nm without the sample, but 1 mL of distilled water made the solution a blank.

The amount of total flavonoids was expressed as rutin equivalents (milligrams of rutin per gram of sample) through the calibration curve of rutin. The structure of rutin is shown in Scheme 2. To determine the working curve of UV absorbency/total flavonoid concentration, the absorbency of the standard rutin solution with different concentrations was determined with UV analysis performed on a PerkinElmer Lambda 17 UV spectrophotometer (PerkinElmer Co.) at a wavelength at 415 nm. The results demonstrated that the working calibration curve showed excellent linearity over the range 0.00788–0.0394 mg/mL. The regression line was as follows:

$$A=32.995C_e+0.0308\left(R^2=0.9990,\ n=5\right)$$

where A is the absorbance of total flavonoids, C_e is the total flavonoid concentration (mg/mL), and R^2 is the correlation coefficient.

Table I. Important Characteristics of DDM1, PPDA, PANP, and PANB

Adsorbent	DDM1	PPDA	PANP	PANB
Matrix	P(St-DVB)	P(St-DVB)	P(St-DVB)	P(St-DVB)
Average pore diameter (Å)	118.9	89.02	86.72	85.0
Total BET surface area (m^2/g)	509.2374	626.3968	621.4504	642.8485
Pore volume (cm^3/g)	1.70	1.394064	1.347251	1.366090
Particle size (mm)	0.2-0.3	0.2-0.3	0.2-0.3	0.2-0.3
Functional group	Chloromethyl	PPDA	PANP	PANB
Group amount (mmol/g)	3.55	0.50	0.49	0.52

*P(St-DVB): Polystyrene-co-divinylbenzene copolymer.

Adsorption and Desorption Kinetics

The adsorption kinetic curves of rutin on the selected modified ones with PPDA, PANP, and PANB groups were studied according to the following process: we added 3.08 g of pretreated resin (equal to 1.0 g of dry resin) and 1000 mL of the sample solution to each flask with a lid. Then, the rutin concentrations in the adsorption process were determined with a UV spectrophotometer at different time intervals until equilibration. Subsequently, the desorption kinetics curves of rutin on the selected modified ones were as follows. After the adsorption reached equilibrium, the adsorbate-laden MARs were put into the flask. A volume of 1000 mL of ethanol (70% v/v) was pumped into each flask. The concentrations of rutin at different time intervals until equilibration were determined by a UV spectrophotometer. In all cases, three parallel measurements were carried out to obtain a mean value, and the standard deviation was less than 3%.

Effect of the Sample Solution pH Value on q_e

The effect of the initial pH on the adsorption of compounds 1, 2, and 3 was studied in the range of pH from 2 to 11; the pH values were adjusted with concentrated hydrochloric acid or NaOH. For these experiments, 100 mL of sample solution was placed in a flask, and 1 g of resin was added. The solution was agitated in a constant-temperature shaker (200 rpm) for 8 h. The adsorption solution was analyzed by a UV spectrometer.

Effect of NaCl and Na_2SO_4 on the Adsorption

The amount of extraction solution and resin was identical to those of the experiments for the pH series. The concentrations of Na_2SO_4 and NaCl were varied from 0 to 10 g/L and 0 to 24 g/L, respectively, and the effect of the solution chemistry on adsorption was conducted at 298 K for 10 h. All of the experiments were repeated three times to obtain average values.

RESULTS AND DISCUSSION

Characterization of the Polymeric Adsorbents

The chlorine content of chloromethylated PS was measured to be 3.55 mmol/g, the corresponding content of the functional groups of PPDA, PANP, and PANB were determined to be 0.50, 0.49, and 0.52 mmol/g, respectively; this implied that the substituted reactions of chloromethylated PS with PPDA, PANP, and PANB were achieved successfully. The results of the nitrogen sorption/desorption analysis are shown in Table I. The specific surface areas of the chloromethylated PS, PPDA, PANP, and PANB were scaled to be 509.2374, 626.3968, 621.4504, and 642.8485 m^2/g, respectively; this revealed that the surface area increased after the functionalized reaction. However, the three synthesized MARs did not bring many differences for the BET specific surface area (Table I). Figure 1 indicates that Friedel–Crafts reaction resulted in a transfer for the pore diameter distribution of the resin. Mesopores and macropores were the main pores for modified PS, and the average pore diameters of PPDA, PANP, and PANB were 9.825, 9.589, and 9.422 nm, respectively. This showed that PPDA had a bit higher proportion of mespores than PANP and PANB. The higher q_e and affinity of PPDA compared to those of PANP and PANB also confirmed the viewpoint mentioned previously.

The IR spectra of the chloromethylated PS, PPDA, PANP, and PANB are shown in Figure 2. After chloromethylated PS reacted with PPDA, there appeared one single moderate peak at the high-wave-number region with a frequency of 3374.3 cm^{-1}, which was assigned to N—H stretching. In addition, C—N stretching was evident at 1024.1 cm^{-1}. Furthermore, two characteristic peaks related to the C=C stretching of the phenyl group at 1605.5 and 1495.2 cm^{-1} were much stronger than before the reaction, and another two bands at 750.3 and 694.6 cm^{-1}, which involved C—H out-of-plane bending for the

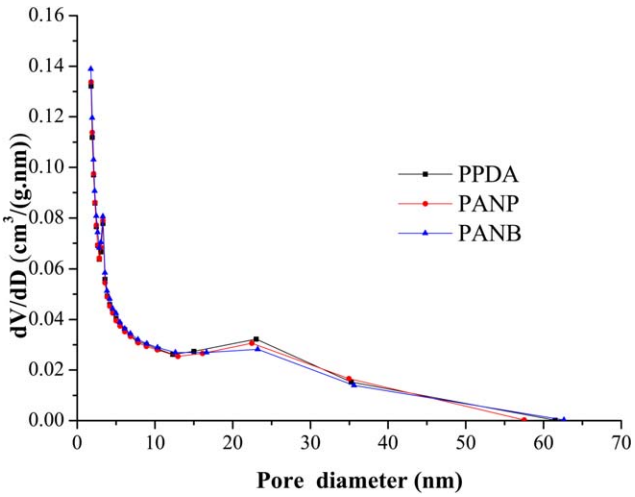

Figure 1. Pore diameter distributions of PPDA, PANP, and PANB, dV/dD (pore volume/pore diameter). [Color figure can be viewed in the online issue, which is available at wileyonlinelibrary.com.]

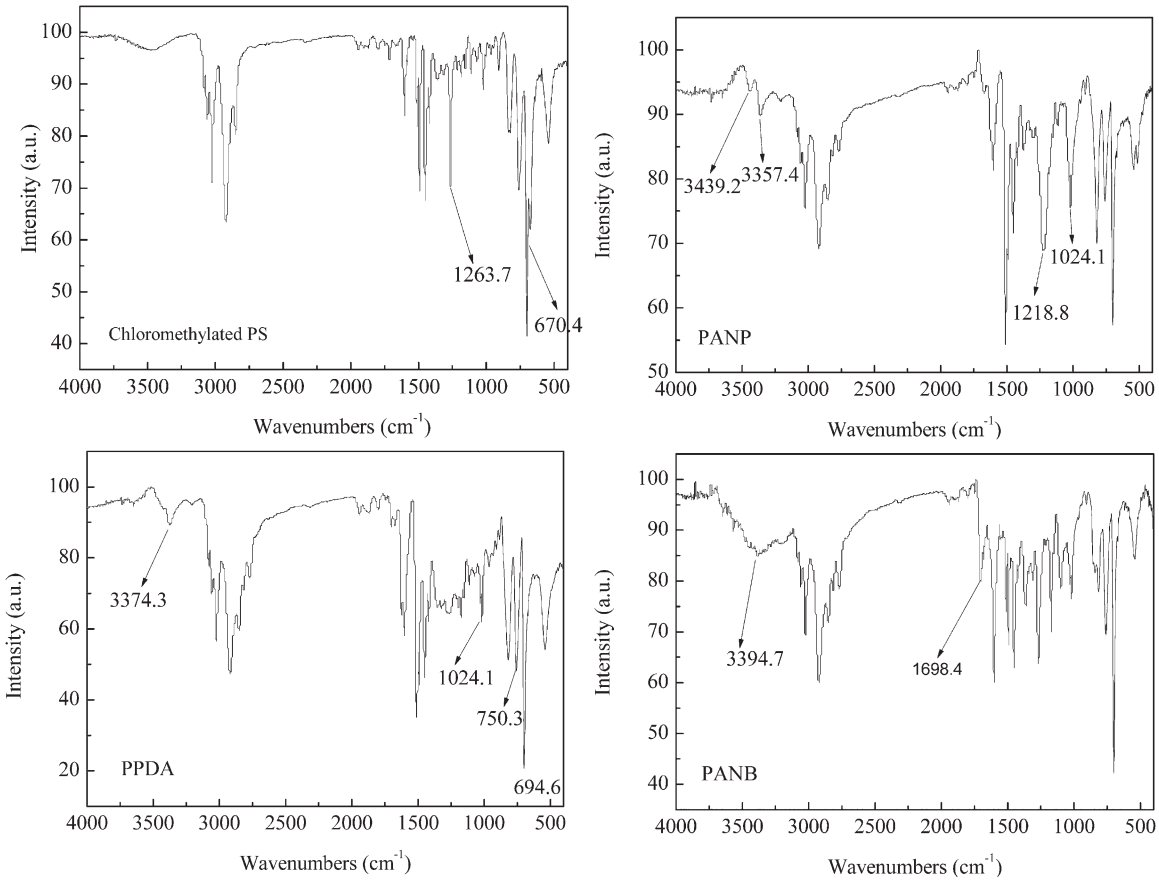

Figure 2. IR spectra of chloromethylated PS, PPDA, PANP, and PANB.

monosubstitution of benzene, were present in the IR spectrum of PPDA. The appearances of these peaks confirmed the successful substituted reaction, and chloromethylated PS reacted with PPDA by equivalent moles.

With regard to the PANP-modified PS, two other moderate peaks of aromatic ether appeared; one was detected at 1218.8 cm^{-1} and was assigned to Ar—O stretching, and the other was measured at 1024.1 cm^{-1} and was related to C—N stretching (Figure 2). The band at 3357.4 cm^{-1} related to N—H vibration indicated that the —NHPhOH group was uploaded on the matrix of the adsorbent. In addition, the C—H bending vibrations of 1,4-disubstituted benzene at 694.6 and 750.3 cm^{-1} were greatly enhanced in contrast with the chloromethylated PS. As a result, the modification of the PANP groups on the matrix of the chloromethylated PS was achieved successfully.

After the substitution reaction, two strong representative peaks related to CH_2Cl groups at 1263.1 and 670.4 cm^{-1} were greatly weakened. This resulted in a few new changes for the IR spectrum of the PANB-modified resin. There was a moderate peak at 1025.3 cm^{-1}, which was assigned to C—N stretching. A moderate C=O stretching band involved in formaldehyde carbonyl groups appeared at 1698.4 cm^{-1}, and the appearance of this band may have resulted from the oxidation of benzyl chloride of chloromethylated PS.[24] Finally, a weak absorption band appeared at 3394.7 cm^{-1}, and this band was related to the O—H stretching of hydroxyl hydrogen.

Adsorption and Desorption Isotherms of the Total Flavonoids of Olive Leaf onto the Three Adsorbents in the Sample Solutions

Figure 3 depicts the adsorption isotherms of the flavonoids onto PPDA, PANP, and PANB in the sample solution. We observed that the equilibrium adsorption isotherms of the total flavonoids were consistent with the type II equilibrium adsorption isotherms classified by Brunauer, which are considered to be multilayer reversible adsorption processes taking place on the solid adsorbent. Additionally, an increase in the reaction temperature from 298 to 318 K observably augmented the adsorption; this was attributed to the fact that the high temperature made the resins swells better. The larger the volume and aperture the resins possessed, the more molecules of rutin entered the resins. Meanwhile, the stereospecific blockade of the adsorption site grew down with the increasing aperture size; thus, the absolute number of adsorption sites increased in the adsorption process. Moreover, the molecular thermodynamic movement of rutin was intense under a higher temperature, and more molecules of rutin got into the aperture of the resins. Therefore, the reaction temperature may have played a dominant role in rutin adsorption on the spent adsorbents.

The q_e values of the flavonoids on the three adsorbents followed the order PPDA > PANP > PANB > DDM0; this suggested that after modification, the synthesized MARs had a better q_e value

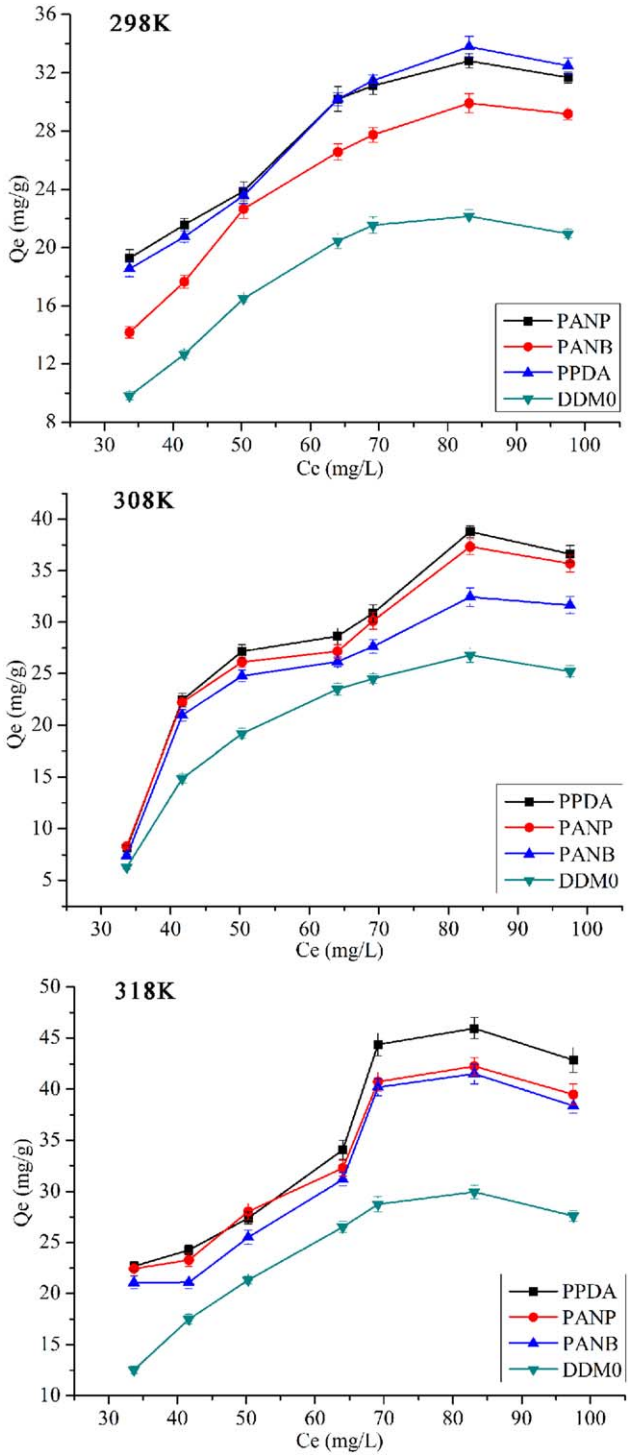

Figure 3. Adsorption isotherms of rutin onto three resins at 298, 308, and 318 K (Qe, the equilibrium adsorption capacity.). [Color figure can be viewed in the online issue, which is available at wileyonlinelibrary.com.]

than DDM0, and the adsorption affinity of PPDA for the total flavonoids was the greatest.

The Langmuir and Freundlich adsorption equations are frequently used to describe the adsorption process.

The Langmuir adsorption equation is[25]

$$\frac{C_e}{q_e} = \frac{C_e}{q_m} + \frac{1}{q_m K_L} \tag{3}$$

where q_m is the maximum adsorption capacity (mg/g) and K_L is a constant.

The Freundlich adsorption equation is[26]

$$\log q_e = \log K_F + \frac{1}{n} \log C_e \tag{4}$$

In the Freundlich adsorption equation, K_F and n are the constants. K_F is an indicator of the adsorption capacity, and n is referred to as the adsorption intensity.

Plotting C_e/q_e against C_e and log q_e versus log C_e with the equilibrium adsorption data would give a straight line, respectively. The regression equations; parameters K_L, K_F, and n; and the R^2 values are summarized in Table II. As shown in Table II, the Freundlich model appeared to fit the equilibrium data better compared with the Langmuir model. It is well know that the Langmuir isotherm is based on the supposition that the surface of the adsorbent has a homogeneous surface, whereas the Freundlich isotherm applies to the adsorption process on a heterogeneous surface. Therefore, the adsorption is a multilayer adsorption process, and the adsorbents possess heterogeneous adsorption sites.

The derivative van't Hoff equation states[27,28]

$$\ln C_e = \frac{\Delta H}{RT} + \ln K \tag{5}$$

where T is the absolute temperature, R is the ideal gas constant, ΔH is the isosteric adsorption enthalpy (kJ/mol), and K is a constant. From eq. (5), ΔH can be figured out from the adsorption isosters with the plot of ln C_e versus $1/T$, as shown in Figure 4.

The adsorption free energy (ΔG; kJ/mol) can be calculated from eq. (6):[29]

$$\Delta G = -nRT \tag{6}$$

where n is the characteristic constant in the Freundlich adsorption equation in Table II.

The adsorption entropy (ΔS) can then be obtained by the Gibbs–Helmholtz equation:

$$\Delta S = \frac{(\Delta H - \Delta G)}{T} \tag{7}$$

The ΔH, ΔG, and ΔS values of the flavonoids onto the three adsorbents are presented in Table III. All of the ΔH values were negative, and this showed an exothermic process. ΔH decreased with increasing total flavonoid uptakes onto the PPDA. This resulted from the surface energy heterogeneity of PPDA.[30] The ΔH values were in the range of 20–50 kJ/mol; this implied that the adsorption was a physical process. ΔG was also negative, indicating that the adsorption was favorable and spontaneous. In addition, it was independent of q_e and changed little when the temperature was altered. The negative ΔS suggested that a more ordered arrangement of flavonoids molecules was shaped

Table II. Fits of the Langmuir and Freundlich Isotherms and Parameters of the Isotherms for the Three Different Resins

T (K)	Regression equation: Langmuir isotherm equation	K_L	q_m	R^2
298 (PPDA)	$y = 0.0158x + 1.2569$	0.0126	63.291	0.8708
298 (PANP)	$y = 0.0184x + 1.0915$	0.0169	54.347	0.9121
298 (PANB)	$y = 0.0144x + 1.6636$	0.0087	69.444	0.7396
308 (PPDA)	$y = 0.0151x + 1.3075$	0.01155	66.225	0.8929
308 (PANP)	$y = 0.0158x + 1.336$	0.01183	63.2911	0.8888
308 (PANB)	$y = 0.0208x + 1.177$	0.01767	48.0769	0.9682
318 (PPDA)	$y = 0.0097x + 1.4066$	0.0069	103.093	0.7073
318 (PANP)	$y = 0.0127x + 1.2963$	0.0098	78.7401	0.8336
318 (PANB)	$y = 0.0111x + 1.5257$	0.00728	90.0901	0.6954
T (K)	Freundlich isotherm equation	K_F	n	R^2
298 (PPDA)	$y = 0.6109x + 0.3426$	2.2009	1.6369	0.9267
298 (PANP)	$y = 0.5398x + 0.4702$	2.9525	1.8525	0.9159
298 (PANB)	$y = 0.7148x + 0.0995$	1.2445	1.1058	0.9093
308 (PPDA)	$y = 0.5229x + 0.4884$	3.0789	1.9124	0.9403
308 (PANP)	$y = 0.6737x + 0.265$	2.9868	1.8736	0.9449
308 (PANB)	$y = 0.4378x + 0.6117$	4.0898	2.2842	0.9677
318 (PPDA)	$y = 0.6775x + 0.2697$	1.8608	1.4760	0.9182
318 (PANP)	$y = 0.6036x + 0.3855$	2.4294	1.6567	0.9229
318 (PANB)	$y = 0.6669x + 0.2468$	1.7652	1.4995	0.9024

on the PANB surface after adsorption. From Table III, we can figure out that the absolute value of ΔS of PANP was the largest; this means that the adsorption of MAR with the functional group (PPDA) was the most disordered arrangement.

In addition, the adsorption isotherms of flavonoids onto the three adsorbents at 298, 308, and 318 K were compared. As shown in Figure 3, the q_e values of the flavonoids onto PANP and PANB were smaller than those of PPDA at the same temperature and C_e. The reason was not only the interaction between the functional groups of the resins and weak-acid flavonoids but also its surface area and pore structure. Its ΔH was measured to be -44.91 kJ/mol. The q_e' values of the three MARs are shown in Figure 5. It was clear that PPDA also released the flavonoids easily. This result may have been because of the following reasons. The amino functional group was an electron-donating group and led to an increased electronic density of the nitrogen atom, and its hydrogen-bonding ability as a hydrogen-bonding acceptor was strengthened. Meanwhile, the electronic density of the benzene ring also increased because of its electron-donating properties, and its hydrogen-bonding ability also increased.

The benzene ring of the adsorbents interacted with the phenyl group of the flavonoids adsorbed onto the adsorbents via π–π stacking, and π–π stacking was also probably responsible for the adsorption. As a result, the adsorption was a synergistic effect. Except for the hydrogen bonding, π–π stacking derived from the benzene ring of the three adsorbents and the phenyl group of the flavonoids may also have been a factor we needed to take into account.[31]

The adsorbent with carbonyl groups had the lowest q_e in the three types of adsorbents; this may have been because the carbonyl group had the poor ability to form hydrogen-bonding interactions.

Perhaps the amino group in the adsorbent produced acid–alkaline interactions with the acid phenolic hydroxyl group in the flavonoids. So, we concluded that the adsorbent with amino groups was more suitable to adsorb flavonoids than the adsorbent with hydroxyl groups.

Adsorption and Desorption Kinetic Curves

As shown in Figure 6, the adsorption and desorption reached equilibrium within 500 min. It was clear that the PPDA not only adsorbed a larger quantity of flavonoids but also released flavonoids efficiently compared to the other two resins. To better illustrate the adsorption properties of the synthetic copolymer, the equilibrium adsorption kinetics of rutin on the synthetic MAR resin was investigated at 308 K.

In general, the pseudo-second-order rate equation is appropriate for the whole adsorption process. Hence, in this study, we used it to fit the adsorption kinetic data. Its linear form is[32]

$$\frac{t}{q_t} = \frac{1}{k_2 q_e^2} + \frac{t}{q_e} \tag{8}$$

where k_2 is the pseudo-second-order rate constant (g $mg^{-1}\cdot min^{-1}$). In Table IV, it is shown that the pseudo-second-order rate equation characterized the adsorption well with $R^2 > 0.9$. In particular, k_2 increased with increasing temperature of the solutions. In particular, the adsorption at a higher

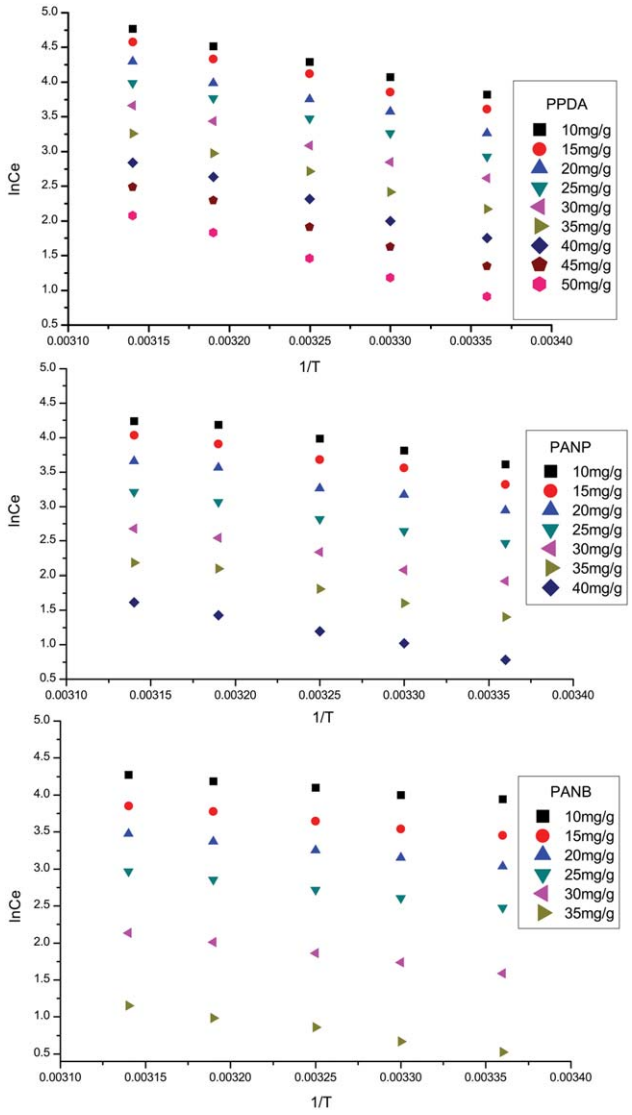

Figure 4. Adsorption isosters of flavonoids adsorbed onto PPDA, PANP, and PANB. [Color figure can be viewed in the online issue, which is available at wileyonlinelibrary.com.]

temperature had a greater k_2, in accordance with the previous observation that the required time at a higher temperature was shorter.

In addition, the initial adsorption rate (h; mg $g^{-1}\cdot min^{-1}$) and half-adsorption time ($t^{1/2}$; min) could be calculated as follows:

$$h = k_2 q_e^2 \tag{9}$$

$$t_{\frac{1}{2}} = \frac{1}{k_2 q_e} \tag{10}$$

As shown in Figure 7, h at a higher temperature was greater, and the required $t^{1/2}$ at a higher temperature was much shorter.

In common, intraparticle diffusion is the rate-limiting step for the adsorption of a hypercrosslinked resin toward aromatic compounds from aqueous solution.[33] Therefore, the kinetic data are further dealt with by the intraparticle diffusion model proposed by Weber and Morris:[34]

$$q_t = k_d t^{\frac{1}{2}} + C \tag{11}$$

where k_d is the intraparticle diffusion rate (mg $g^{-1}\cdot min^{-1/2}$) and C is a constant. When the solid-phase sorbate concentration at a given time (q_t) versus $t^{1/2}$ is plotted and it gives a straight line, the straight line passes through the origin, and the intraparticle diffusion is the rate-limiting step for the adsorption. If it presents a multilinear relationship or does not pass through the origin, two or more diffusion mechanisms affect the adsorption.[35] With the plotting of q_t versus $t^{1/2}$ for the adsorption, it was found that they yielded a multistage process. At the initial stage, it posed a linear relationship, and the straight lines passed through the origin; this indicated that the intraparticle diffusion was the rate-limiting step. Moreover, k_{d1} presented the order k_{d1} (298 K) $< k_{d1}$ (308 K) $< k_{d1}$ (318 K); this implied that the adsorption rate at a higher temperature was greater. In the second stage, plots of q_t versus $t^{1/2}$ also yielded linear relationships but did not pass through the origin. This revealed that multidiffusion mechanisms were involved.

Effect of the Initial Sample Solution pH on the Adsorption Capacity

The pH value of the sample solution was very important for the adsorption and desorption properties of the resins because the pH value determined the extent of ionization of solute molecules and thereby affected their adsorption affnity.[36] The flavonoids of the *O. europaea L.* leaves are weakly acidic compounds because of the existence of phenolic hydroxyl groups. The pH value of the extract solution was 4.6, and the pK_a value was 7.3. According to the results shown in Figure 8, the highest q_e values of PPDA, PANP, and PANB for the flavonoids of the *O. europaea L.* leaves were 5, 5.5, and 6, respectively; these values decreased with increasing pH value. At higher pH values of 8–11, the q_e values of the flavonoids on the three resins decreased rapidly. These observations suggested that hydrogen bonding might have played a key role in the adsorption process of the three resins. At higher pH values, the hydrogen-bonding interactions decreased because the phenolic hydroxyl groups in the flavonoids dissociated to form H^+ and their corresponding anions; this resulted in a decrease in q_e. At lower pH values, the surface of the resins was surrounded by the hydronium ions; this enhanced the interaction of the un-ionized phenolic hydroxyl groups of the flavonoids with the resins by potent attractive forces. Hence, the pH value of sample solution was adjusted to 5.5 for all later experiments.

Effect of NaCl and Na_2SO_4 on Adsorption

The effect of certain salts on the anion-exchange process is known as the *competition effect*, which causes a decline in the exchange capacity for anion contaminants.[37,38] However, the effect of sodium sulfate and sodium chloride on the adsorption ability of three resins for flavonoids was determined in this study. The concentration range of Na_2SO_4 was from 0 to 10 g/L, whereas the concentration range of NaCl was from 0 to 24 g/L. The results are shown in Figure 9. We observed that sodium sulfate affected the adsorption slightly. However, the q_e values of

Table III. Adsorption Thermodynamic Parameters of Flavonoids Adsorbed onto Three Different Resins

			ΔG (kJ/mol)			ΔS (J/mol)		
	q (mg/g)	ΔH (kJ/mol)	298 K	308 K	318 K	298 K	308 K	318 K
PPDA	50	−35.285	−4.056	−4.897	−3.902	−132.01	−130.46	−123.23
	45	−36.399	−4.056	−4.897	−3.902	−135.75	−134.08	−126.73
	40	−37.463	−4.056	−4.897	−3.902	−139.32	−137.53	−130.08
	35	−39.799	−4.056	−4.897	−3.902	−147.16	−145.12	−137.42
	30	−40.564	−4.056	−4.897	−3.902	−149.73	−147.60	−139.83
	25	−41.237	−4.056	−4.897	−3.902	−151.99	−149.79	−141.95
	20	−42.443	−4.056	−4.897	−3.902	−156.04	−153.70	−145.74
	15	−44.538	−4.056	−4.897	−3.902	−163.07	−160.50	−152.33
	10	−44.962	−4.056	−4.897	−3.902	−164.49	−161.88	−153.66
PANP	40	−24.651	−4.590	−4.798	−4.380	−98.12	−95.61	−91.29
	35	−26.946	−4.590	−4.798	−4.380	−105.82	−103.06	−98.51
	30	−27.677	−4.590	−4.798	−4.380	−108.28	−105.44	−100.81
	25	−28.625	−4.590	−4.798	−4.380	−111.46	−108.52	−103.79
	20	−29.939	−4.590	−4.798	−4.380	−115.87	−112.78	−107.92
	15	−31.078	−4.590	−4.798	−4.380	−119.69	−116.48	−111.50
	10	−31.493	−4.590	−4.798	−4.380	−121.08	−117.83	−112.81
PANB	35	−12.779	−2.740	−5.849	−3.964	−52.07	−60.48	−52.65
	30	−15.605	−2.740	−5.849	−3.964	−61.56	−69.66	−61.54
	25	−16.670	−2.740	−5.849	−3.964	−65.13	−73.11	−64.89
	20	−18.615	−2.740	−5.849	−3.964	−71.66	−79.43	−71.00
	15	−20.561	−2.740	−5.849	−3.964	−78.19	−85.75	−77.12
	10	−23.712	−2.740	−5.849	−3.964	−88.76	−95.98	−87.03

*q:The adsorption capacity

the three resins were enhanced with increasing concentration of NaCl. When the concentration of the salts increased beyond this range, the q_e values stabilized at the maximum. There was no obvious change for the NaCl concentration over 20 g/L. The adsorption was enhanced with increasing concentration of salt, and this might have contributed to the effect of salting out. In the salt extraction solution system, the salt ions were covered with water (H_2O) molecules, and this led to a high concentration of flavonoids in solution far from the ions. Furthermore, the adsorbed flavonoids might have prevented ions from moving into the resin, and the hydrophobic interaction between the absorbed flavonoids and dissolved flavonoids was improved because the interactions between water molecules were enhanced by the effect of NaCl. The repulsion between the adsorbed flavonoids and dissolved flavonoids might have served to oppose adsorption. The salts interacted with the adsorbate and screened the repulsive forces. Because of the possible competition effect on the surface of resin, the maximum flavonoid q_e caused by Na_2SO_4 was lower than that of NaCl.

Comparison of the Adsorption Capacity of the Flavonoids onto Resins with Different Additions of Hydrogen Reagent (HR)

The adsorption capacities of the flavonoids onto different contents of HR-modified resins, including HR-02, HR-04, HR-05, HR-06, HR-08, and HR-10, were first compared, and the results are displayed in Figure 10. The q_e values of the flavonoids on HR-05 was the largest among the four resins, and hence, HR-05 was used as a specific polymeric adsorbent in this study. The possible reason for the this observation may have been the chemical modification of the hydrogen-bonding groups on the surface of the resin. With increasing amount of functional groups reacted, a lot of pores in the resins collapsed after drying. The swelling ratio of the resins in water increased somewhat with the introduction of hydrogen-bonding groups; this implied that the flexibility of the polymer chain in polar solvents increased with the introduction of hydrogen-bonding groups, and thus, the pores of the synthesized resin more easily collapsed as the resin was dried; this led to a decrease in the specific surface area of the dried synthesized resin and thus affected the adsorbent capacity.

Adsorption Mechanism of the Flavonoid Constituents from the Leaves of *O. europaea L* onto the Three Adsorbents in the Sample Solutions

In this study, FTIR spectroscopy was used to examine the existence of amino, hydroxyl, and carbonyl groups on the functionalized resin. The vibrational frequency in the FTIR spectrum is sensitive to changes in chemical bonds; a slight interaction change between the adsorbent and the adsorbate will bring on

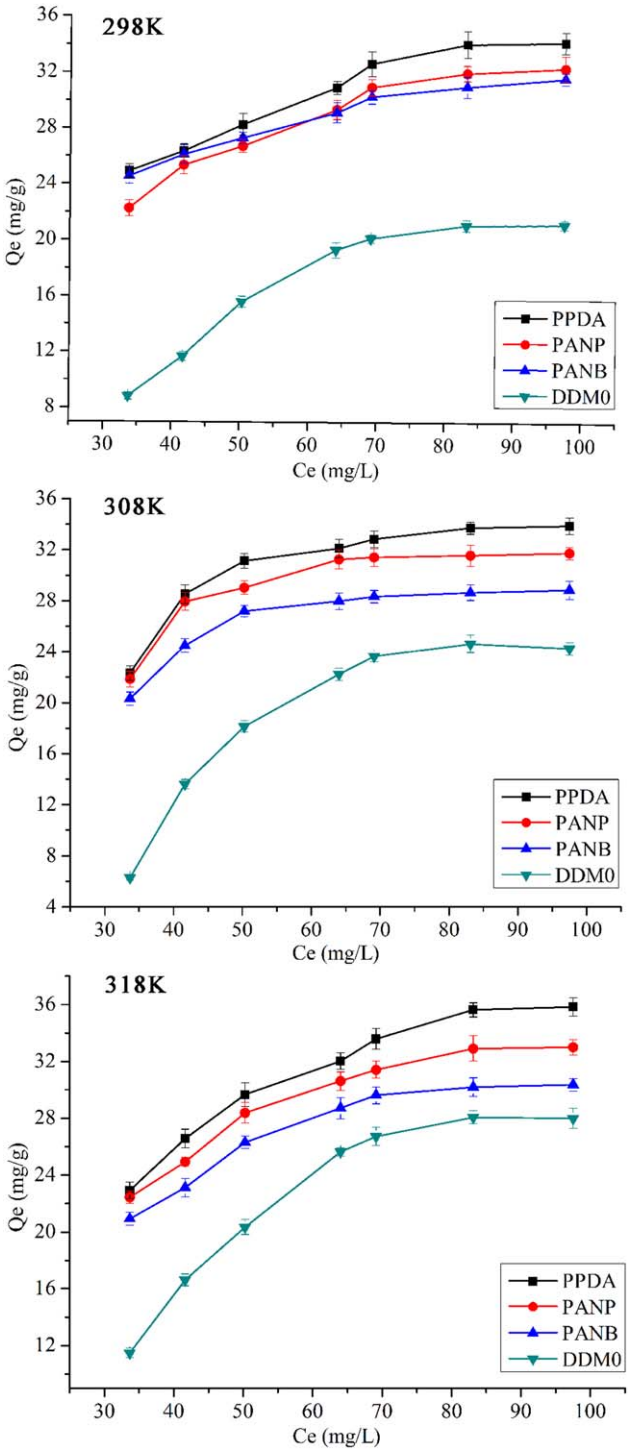

Figure 5. Desorption isotherms of rutin onto three resins at 298, 308, and 318 K. [Color figure can be viewed in the online issue, which is available at wileyonlinelibrary.com.]

several vibrational shifts.[39] In this study, FTIR spectroscopy was used to examine the shifts of formaldehyde carbonyl and quinone carbonyl groups on the resin so that the adsorption mechanism could be clarified. The typical results of the synthesized resins after the adsorption of flavonoids are depicted in Figure 11. The main peak at 3410 cm^{-1} appeared and was assigned to

Table IV. Parameters of the Pseudo-Second-Order Rate Equation

	Pseudo-second-order rate equation	q_e	k_2	R^2
PPDA	$y = 0.0649x + 1.1426$	15.4083	0.003686	0.9953
PANP	$y = 0.0890x + 0.5790$	11.236	0.01368	0.9997
PANB	$y = 0.0701x + 0.8978$	14.2653	0.005473	0.9981

hydroxyl groups after the adsorption of flavonoids. The characteristic vibration of flavonoids also appeared. Commonly, the formation of hydrogen bonding leads some characteristic bands to widen. We can see this in Figure 11. So, we deduced that hydrogen bonding appeared to be one of the primary driving forces for the adsorption of flavonoids onto the synthesized resins, and hydrogen bonding is one of the primary driving forces for the adsorption. In addition, π–π stacking between the benzene ring of the adsorbents and the phenyl group of the flavonoids was also a factor in the adsorption process. Furthermore, hydrophobic interaction could not be ignored for the adsorption process in this study. So, the adsorption mechanism of this

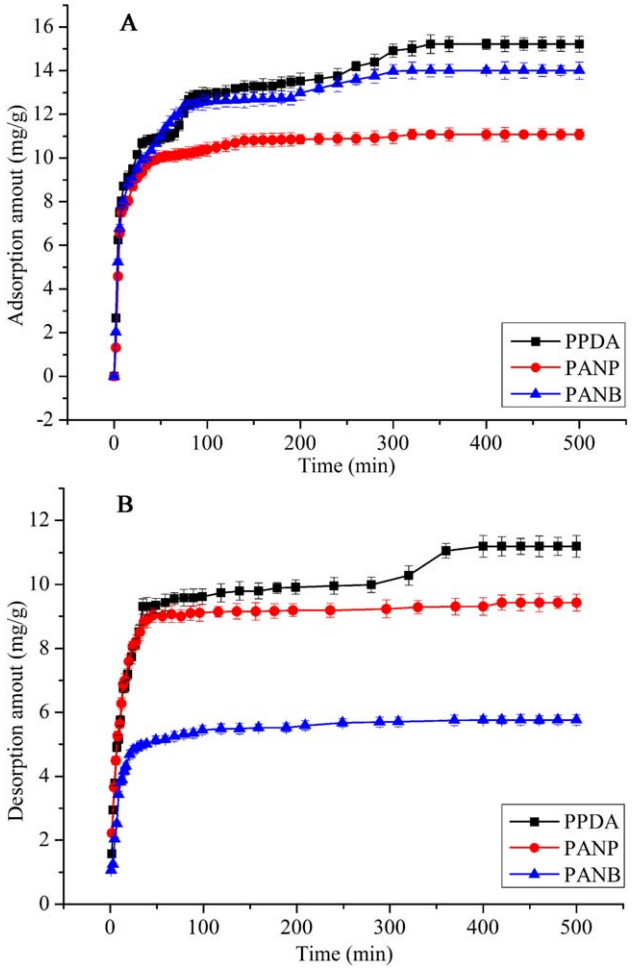

Figure 6. (A) Adsorption and (B) desorption kinetic curves of rutin on different MARs at 308 K. [Color figure can be viewed in the online issue, which is available at wileyonlinelibrary.com.]

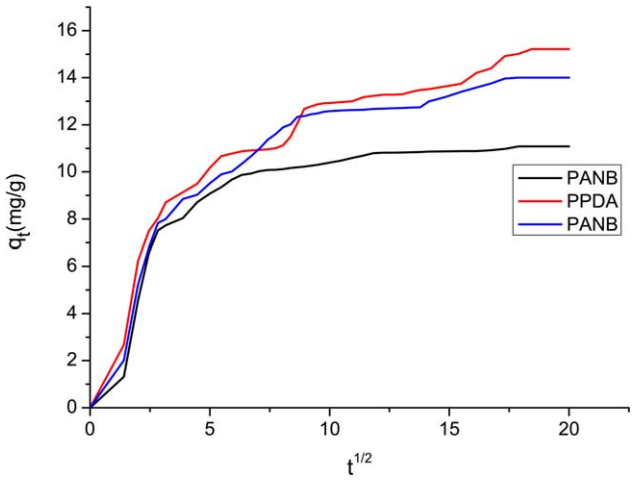

Figure 7. Intraparticle diffusion model of the three resins. [Color figure can be viewed in the online issue, which is available at wileyonlinelibrary.com.]

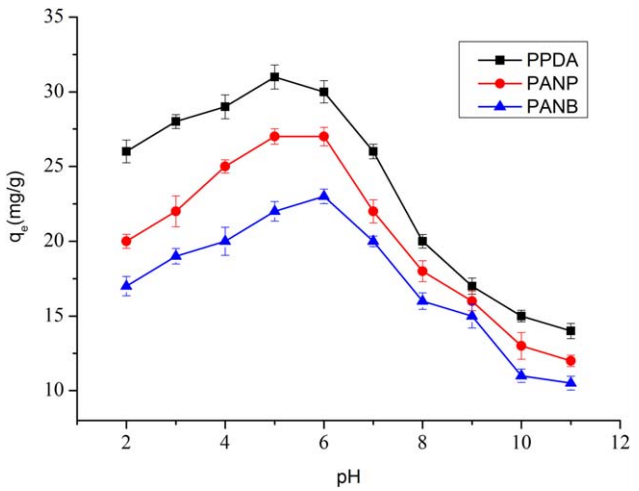

Figure 8. Effect of the initial sample solution pH value on q_e. [Color figure can be viewed in the online issue, which is available at wileyonlinelibrary.com.]

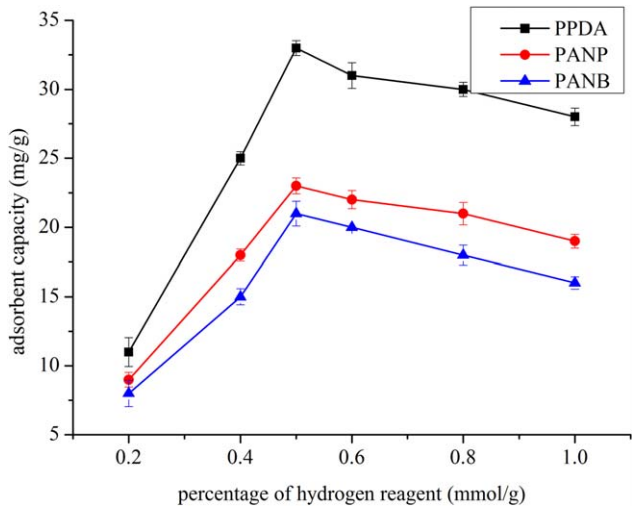

Figure 10. Comparison of q_e of flavonoids onto resins with different additions of HR. [Color figure can be viewed in the online issue, which is available at wileyonlinelibrary.com.]

study was attributed to the synergistic effect of hydrogen bonding, π–π stacking, and hydrophobic interactions.

PPDA had the largest q_e in comparison with the others; this was ascribed to the fact that it had a comparatively strong ability to form hydrogen bonds with the flavonoids. Moreover, the amino group in the PPDA produced acid–alkaline interactions with the acid phenolic hydroxyl groups in the flavonoids of *O. europaea L.* Meanwhile, the electronic density of the benzene ring differed according to the electronic-donating and electronic-withdrawing functional group. It is well known that polarity matching between the adsorbent and the adsorbate plays an important role in the adsorption process. In common, polar adsorbents selectively adsorb polar adsorbates. The adsorbent modified by PPDA had the strongest polarity of the three types of adsorbents. Hence, the adsorption affinity of flavonoids with PPDA was higher than those of the others. In the tested system, polarity matching between the PPDA and flavonoids should have been displayed by hydrogen bonding. The BET surface area and the porous structural parameters of the synthesized MARs were

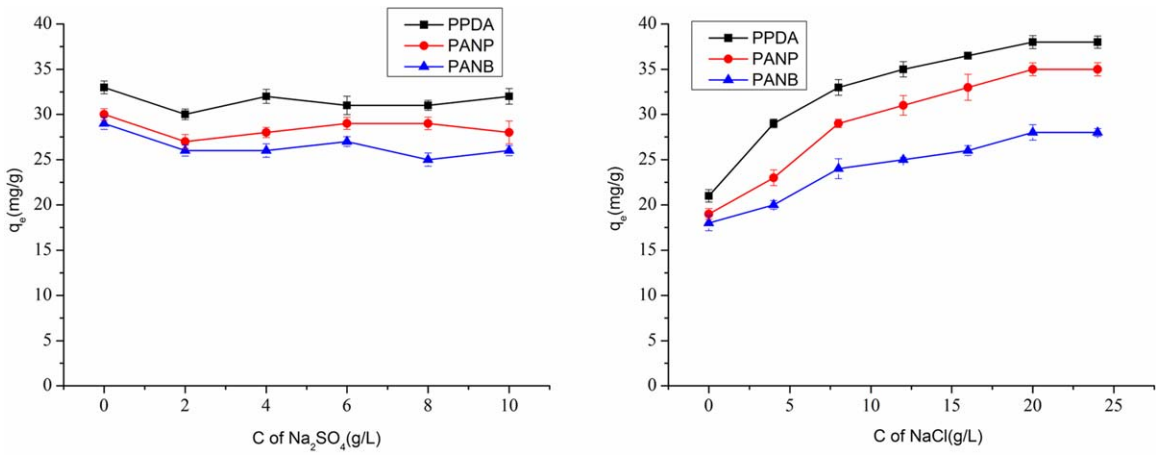

Figure 9. Effect of Na_2SO_4 and NaCl on adsorption. [Color figure can be viewed in the online issue, which is available at wileyonlinelibrary.com.]

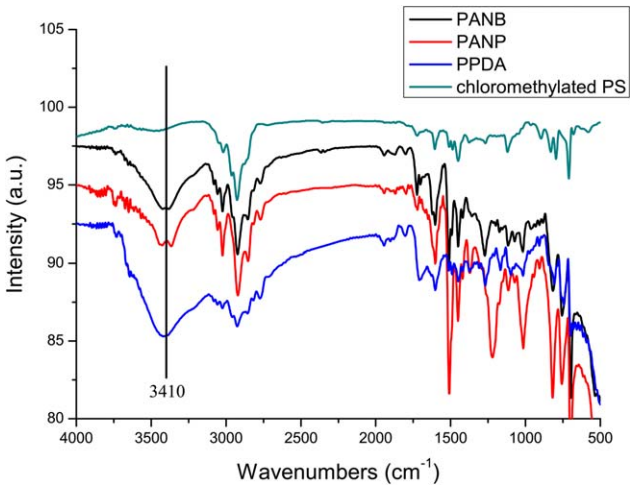

Figure 11. IR spectra of the resins after the adsorption of the flavonoids. [Color figure can be viewed in the online issue, which is available at wileyonlinelibrary.com.]

close to each other, so the large difference in q_e could not be explained from the small difference in the BET surface area. However, the distribution of the pore diameter may have had a little influence on the adsorption. Therefore, the match between the pore diameter of the MARs and the molecular size of the flavonoids was also a factor that was noted.

CONCLUSIONS

A series of novel MARs of PPDA, PANP, and PANB with different functional groups were synthesized successfully. They could efficiently adsorb flavonoids of *O. europaea L.*,[40–42] and PPDA had the highest q_e. The Freundlich model depicted the isotherms better than the Langmuir model; this suggested that the surface energy of the adsorbent was inhomogeneous. The adsorption was shown to be an exothermic, spontaneous, and more ordered arrangement process from the measured ΔH, ΔG, and ΔS. The pseudo-second-order rate equation was suitable to fit the adsorption dynamic curve. The effect of the sample solution pH value on q_e showed that hydrogen bonding played an important role in the interaction. Hydrogen bonding between the nitrogen atom of the amino group, the oxygen atom of the hydroxyl group, the carbonyl group of the adsorbent, and the hydrogen atom of the hydroxyl group of the flavonoids was principally responsible for the adsorption of the flavonoids. The possible adsorption mechanism was the synergistic effect of hydrogen bonding, π–π stacking, and hydrophobic interaction. In addition, the difference in the electronic densities of the functional groups in the adsorbents and the acid–alkaline interaction between the adsorbents and adsorbates also influenced the adsorption. The structures of the effective components in natural plants are complicated and multiform, and many kinds of weak interactions exist. As a result, the synergistic effect of multiweak interactions should be universal in the adsorption mechanism, and more adsorbents can be designed on this basis. Therefore, control of the adsorbent structure should be important not only in the separation of flavonoids in the leaves of *O. europaea L.* but also in the separation of the more active components in other natural plants.

ACKNOWLEDGMENTS

The authors are grateful for the financial support of the National Natural Science Foundation of China (contract grant number 20974116).

REFERENCES

1. Tsyurupa, M. P.; Malsova, L. A.; Andreeva, A. I.; Mrachkovskaya, T. A.; Davankov, V. A. *React. Polym.* **1995**, *25*, 69.
2. Malik, D. J.; Warwick, G. L.; Venturi, M.; Streata, M.; Hellgardta, K.; Hoenichc, N.; Daled, J. A. *Biomaterials* **2004**, *24*, 2933.
3. Yu, Y.; Zhuang, Y. Y.; Wang, Z. H.; Qiu, M. Q. *Ind. Eng. Chem. Res.* **2003**, *42*, 6898.
4. Du, X. L.; Yuan, Q. P.; Li, Y.; Zhou, H. H. *Chem. Eng. Technol.* **2008**, *31*, 87.
5. Huang, J. H.; Zhou, Y.; Huang, K. L.; Liu, S. Q.; Luo, Q.; Xu, M. C. *J. Colloid Interface Sci.* **2007**, *316*, 10.
6. Huang, J. H.; Huang, K. L.; Liu, S. Q.; Luo, Q.; Shi, S. Y. *J. Colloid Interface Sci.* **2008**, *317*, 434.
7. Yang, W. B.; Li, A. M.; Fan, J.; Yang, L. C.; Zhang, Q. X. *Chemosphere* **2006**, *64*, 984.
8. Li, Y.; Long, C.; Tao, W. H.; Li, A. M.; Zhang, Q. X. *J. Chem. Eng. Data* **2010**, *55*, 3147.
9. Li, H. T.; Hao, Y. C.; Xu, M. C.; Shi, Z. Q.; He, B. L. *Polymer* **2004**, *45*, 181.
10. Pan, B. J.; Zhang, W. M.; Pan, B. C.; Qiu, H.; Zhang, Q. R.; Zhang, Q. X.; Zheng, S. R. *Environ. Sci. Technol.* **2008**, *42*, 7411.
11. Zhang, W. M.; Hong, C. C.; Pan, B. C.; Xu, Z. W.; Zhang, Q. J.; Lv, L. *J. Hazard. Mater.* **2008**, *158*, 293.
12. Chanda, M.; Rempel, G. L. *Ind. Eng. Chem. Res.* **2001**, *40*, 1624.
13. Silva, E. M.; Pompeu, D. R.; Larondelle, Y.; Rogez, H. *Sep. Purif. Technol.* **2007**, *53*, 274.
14. Wang, H. Y.; Zhao, M. M.; Yang, B.; Jiang, Y. M.; Rao, G. H. *Food Chem.* **2008**, *107*, 1399.
15. Zeng, Y.; Li, L.; Yuan, S. D. *Chin. J. Appl. Chem.* **2009**, *26*, 37.
16. Ye, J. H.; Jin, J.; Liang, H. L.; Lu, J. L.; Du, Y. Y.; Zheng, X. Q.; Liang, Y. R. *Bioresour. Technol.* **2009**, *100*, 622.
17. Kammerer, J.; Boschet, J.; Kammerer, D. R.; Carle, R. *LWT—Food Sci. Technol.* **2011**, *44*, 1079.
18. Liu, Y. F.; Liu, J. X.; Chen, X. F.; Liu, Y. W.; Di, D. L. *Food Chem.* **2010**, *123*, 1027.
19. Chen, Z.; Zhang, A.; Li, J.; Dong, F.; Di, D.; Wu, Y. *J. Phys. Chem. B* **2010**, *114*, 4841.
20. Lou, S.; Di, D. L. *J. Agric. Food Chem.* **2012**, *60*, 6546.
21. Li, C.; Zheng, Y. Y.; Wang, X. F.; Feng, S. L.; Di, D. L. *J. Sci. Food Agric.* **2011**, *91*, 2826.

22. Zhang, X.; Li, A. M.; Jiang, Z. M.; Zhang, Q. X. *J. Hazard. Mater.* **2006**, *137*, 1115.

23. Huang, J. G.; Xu, M. C.; Li, H. T.; Shi, Z. Q.; He, B. L. *Chin. Chem. Lett.* **2003**, *14*, 914.

24. Meng, G. H.; Li, A. M.; Yang, W. B.; Liu, F. Q.; Yang, X.; Zhang, Q. X. *Eur. Polym. J.* **2007**, *43*, 2732.

25. Gaunce, A. P.; Anastassiadis, P. A. *Anal. Biochem.* **1966**, *17*, 357.

26. Walker, E. A.; Morton, P. *Analyst* **1964**, *89*, 512.

27. Li, H. T.; Xu, M. C.; Shi, Z. Q.; He, B. L. *J. Colloid Interface Sci.* **2004**, *271*, 47.

28. Cai, J. G.; Li, A. M.; Shi, H. Y.; Fei, Z. H.; Long, C.; Zhang, Q. X. *J. Hazard. Mater.* **2005**, *124*, 173.

29. Garciadelgado, R. A.; Cotoruelominguez, L. M.; Rodriguez, J. *J. Sep. Sci. Technol.* **1992**, *27*, 975.

30. Huang, J. H.; Huang, K. L.; Liu, S. Q.; Luo, Q.; Xu, M. C. *J. Colloid Interface Sci.* **2007**, *315*, 407.

31. Ersoz, A.; Denizli, A.; Sener, I.; Atilir, A.; Diltemiz, S.; Say, R. *Sep. Purif. Technol.* **2004**, *38*, 173.

32. Koehler, J. A.; Brune, B. J.; Chen, T. H.; Glemza, A. J.; Vishwanath, P.; Smith, P. J.; Payne, G. F. *Ind. Eng. Chem. Res.* **2000**, *39*, 3347.

33. Zheng, K.; Pan, B.; Zhang, Q.; Zhang, W. M.; Pan, B. J.; Han, Y. H.; Zhang, Q. R.; Wei, D.; Cu, Z. W.; Zhang, Q. X. *Sep. Purif. Technol.* **2007**, *57*, 250.

34. Weber, W. J.; Morris, J. C.; Sanit, J.; Div, E. *Am. Soc. Civ. Eng.* **1963**, *89*, 31.

35. Zhu, Z. L.; Li, A. M.; Yan, L.; Liu, F. Q.; Zhang, Q. X. *J. Colloid Interface Sci.* **2007**, *316*, 628.

36. Deng, S.; Yu, Q.; Huang, J.; Yu, G. *Water Res.* **2010**, *5188*, 44.

37. Wang, J.; Zhou, Y.; Li, A.; Xu, L. *J. Hazard. Mater.* **2010**, *1018*, 176.

38. Atia, A. A. *J. Hazard. Mater.* **2006**, *1049*, 137.

39. Koehler, J. A.; Wallace, K. K.; Smith, P. J.; Payne, G. F. *Ind. Eng. Chem. Res.* **1999**, *3076*, 38.

40. Huang, J.; Wang, X.; Wang, X.; Huang, K. *Ind. Eng. Chem. Res.* **2011**, *2891*, 50.

41. Wang, X.; Huang, J.; Huang, K. *Chem. Eng. J.* **2010**, *158*, 162.

42. He, C.; Huang, J.; Yan, C.; Liu, J.; Deng, L.; Huang, K. *J. Hazard. Mater.* **2010**, *634*, 180.